



Characterization of Chloroplastic Fructose 1,6-Bisphosphate Aldolases as Lysine-methylated Proteins in Plants.

Morgane Mininno, Sabine Brugiere, Virginie Pautre, Annabelle Gilgen, Sheng Ma, Myriam Ferro, Marianne Tardif, Claude Alban, Stephane Ravanel

► To cite this version:

Morgane Mininno, Sabine Brugiere, Virginie Pautre, Annabelle Gilgen, Sheng Ma, et al.. Characterization of Chloroplastic Fructose 1,6-Bisphosphate Aldolases as Lysine-methylated Proteins in Plants.. Journal of Biological Chemistry, 2012, 287 (25), pp.21034-44. <10.1074/jbc.M112.359976>. <hal-00702116>

HAL Id: hal-00702116

<https://hal.science/hal-00702116v1>

Submitted on 28 May 2020

HAL is a multi-disciplinary open access archive for the deposit and dissemination of scientific research documents, whether they are published or not. The documents may come from teaching and research institutions in France or abroad, or from public or private research centers.

L'archive ouverte pluridisciplinaire **HAL**, est destinée au dépôt et à la diffusion de documents scientifiques de niveau recherche, publiés ou non, émanant des établissements d'enseignement et de recherche français ou étrangers, des laboratoires publics ou privés.



Copyright - All rights reserved

Characterization of Chloroplastic Fructose 1,6-Bisphosphate Aldolases as Lysine-methylated Proteins in Plants^{*,[5]}

Received for publication, March 13, 2012, and in revised form, April 28, 2012. Published, JBC Papers in Press, April 30, 2012, DOI 10.1074/jbc.M112.359976

Morgane Mininno^{‡§||}, Sabine Brugière^{***§§}, Virginie Pautre^{‡§||}, Annabelle Gilgen^{‡§||}, Sheng Ma^{‡§||},
Myriam Ferro^{***§§}, Marianne Tardif^{***§§}, Claude Alban^{‡§||}, and Stéphane Ravanel^{‡§||1}

From the [‡]INRA, USC1359, F-38054 Grenoble, [§]CNRS, UMR5168, F-38054 Grenoble, the ^{||}Commissariat à l'Energie Atomique, Laboratoire de Physiologie Cellulaire et Végétale, F-38054 Grenoble, the ^{||}Université Joseph Fourier-Grenoble I, UMR5168, F-38041 Grenoble, the ^{**}Commissariat à l'Energie Atomique, Laboratoire Biologie à Grande Echelle, F-38054 Grenoble, ^{††}INSERM, U1038, F-38054 Grenoble, and the ^{§§}Université Joseph Fourier-Grenoble I, U1038, F-38041 Grenoble, France

Background: The protein-lysine methyltransferase LSMT from pea methylates the large subunit of Rubisco.

Results: In *Arabidopsis*, Rubisco is not methylated, and the physiological substrates of the LSMT-like enzyme are chloroplastic aldolases.

Conclusion: LSMT homologs from plants display different substrate specificities, with targets involved in carbon metabolism.

Significance: The study identifies chloroplastic aldolases as new lysine-methylated proteins.

In pea (*Pisum sativum*), the protein-lysine methyltransferase (PsLSMT) catalyzes the trimethylation of Lys-14 in the large subunit (LS) of ribulose 1,5-bisphosphate carboxylase/oxygenase (Rubisco), the enzyme catalyzing the CO₂ fixation step during photosynthesis. Homologs of PsLSMT, herein referred to as LSMT-like enzymes, are found in all plant genomes, but methylation of LS Rubisco is not universal in the plant kingdom, suggesting a species-specific protein substrate specificity of the methyltransferase. In this study, we report the biochemical characterization of the LSMT-like enzyme from *Arabidopsis thaliana* (AtLSMT-L), with a focus on its substrate specificity. We show that, in *Arabidopsis*, LS Rubisco is not naturally methylated and that the physiological substrates of AtLSMT-L are chloroplastic fructose 1,6-bisphosphate aldolase isoforms. These enzymes, which are involved in the assimilation of CO₂ through the Calvin cycle and in chloroplastic glycolysis, are trimethylated at a conserved lysyl residue located close to the C terminus. Both AtLSMT-L and PsLSMT are able to methylate aldolases with similar kinetic parameters and product specificity. Thus, the divergent substrate specificity of LSMT-like enzymes from pea and *Arabidopsis* concerns only Rubisco. AtLSMT-L is able to interact with unmethylated Rubisco, but the complex is catalytically unproductive. Trimethylation does not modify the kinetic properties and tetrameric organization of aldolases *in vitro*. The identification of aldolases as methyl proteins in *Arabidopsis* and other species like pea suggests a role of protein lysine methylation in carbon metabolism in chloroplasts.

Protein-lysine methyltransferases (PKMTs)² catalyze the methylation of the ϵ -amine of specific lysyl residues in target

proteins. These enzymes are capable of adding up to three methyl groups originating from S-adenosylmethionine (AdoMet) to form mono-, di-, and trimethylated Lys derivatives. Most of the PKMTs characterized so far contain an evolutionarily conserved catalytic domain named SET, from the three founding *Drosophila* proteins in which it was discovered (Suppressor of variegation 3–9, Enhancer of zeste, and Trithorax) (1). Most SET domain methyltransferases are known to modify histones and to play an important role in epigenetic mechanisms, through changes in chromatin structure and recruitment of chromatin-modifying effectors. Protein Lys methylation extends beyond nucleosome components, and an increasing number of non-histone proteins bearing methyl-Lys residues is being identified in prokaryotes and eukaryotes. These methyl proteins are involved in almost all basic cellular processes, including transcriptional regulation, translation, cellular signaling, and metabolism (2, 3). Also, modifications of lysyl residues by methyl groups were found reversible through the action of demethylases, emphasizing the plasticity and dynamic nature of Lys methylation (3). In most cases, the biological significance of non-histone proteins methylation is poorly understood. Indeed, mutations in genes coding PKMTs specific for non-histone substrates usually do not cause obvious biological or developmental defects.

Plant genomes contain nearly 50 genes coding SET domain proteins, which can be grouped in different classes according to the organization of their SET domains and surrounding motifs (1, 4, 5). This classification is assumed to reflect protein substrate specificity, and members of one class with interrupted SET domains may be involved in modification of non-histone targets. A member of this class located in the chloroplasts of higher plants has been extensively studied in pea (for reviews, see Ref. 2, 6). The enzyme catalyzes the trimethylation of Lys-14 in the large subunit of ribulose 1,5-bisphosphate carboxylase/

^{*} This work was supported by the Department of Plant Biology INRA, the Cluster 9 of the Région Rhône-Alpes, and the French National Research Agency Chloro-Pro Project Blanc SVSE6, 2010.

^[5] This article contains supplemental Figs. 1–4 and Table 1.

¹ To whom correspondence should be addressed. Tel.: 33-438783383; Fax: 33-438785091; E-mail: stephane.ravanel@cea.fr.

² The abbreviations used are: PKMT, protein-lysine methyltransferase; AdoMet, S-adenosylmethionine; FBA, fructose 1,6-bisphosphate aldolase;

FBP, fructose 1,6-bisphosphate; γ TMT, γ -tocopherol methyltransferase; LSMT, large subunit Rubisco methyltransferase; LS Rubisco, large subunit of ribulose 1,5-bisphosphate carboxylase/oxygenase; AtLSMT, *A. thaliana* LSMT; PsLSMT, *P. sativum* LSMT; qPCR, quantitative PCR.

oxygenase (LS Rubisco), the enzyme involved in photosynthetic CO₂ fixation. This SET domain protein is referred to as PsLSMT for *Pisum sativum* LS Rubisco methyltransferase. Genes coding homologs of PsLSMT are found in all plant genomes. However, methylation at Lys-14 was not observed in all the plant species examined. Accordingly, trimethylated Lys-14 was detected in legumes (pea, soybean, and cowpea), Solanaceae (tomato, potato, pepper, tobacco, and petunia), and Cucurbitaceae (cucumber and muskmelon), whereas unmethylated forms of Rubisco naturally occur in spinach and wheat (7). The physiological function of Rubisco methylation is still unknown. Indeed, stoichiometric methylation of spinach Rubisco by PsLSMT *in vitro* does not alter any of the kinetic and activation parameters of the enzyme (2). Also, tobacco plants knocked down for LSMT gene expression displayed no growth phenotype and no difference in CO₂ assimilation rates as compared with wild-type plants (2).

The existence of genes coding LSMT homologs in species with unmodified Lys-14 in LS Rubisco is still an enigma. It has been suggested that the protein substrate specificity of LSMT-like enzymes could vary in a species-specific manner (2, 6). To support this assumption, the chloroplastic enzyme γ -tocopherol methyltransferase (γ TMT) was identified as an alternative substrate of PsLSMT, at least *in vitro* (8). The biochemical and physiological consequences of γ TMT methylation are still unknown.

In this work, we report the biochemical characterization of the LSMT-like enzyme from the model plant *Arabidopsis thaliana* (AtLSMT-L), and we show that this enzyme exhibits protein substrate specificity different from that of PsLSMT. First, we found that LS Rubisco is not naturally methylated at Lys-14 in *Arabidopsis* and that AtLSMT-L interacts with unmethylated Rubisco in a catalytically unproductive way. Second, we identified chloroplastic isoforms of fructose 1,6-bisphosphate aldolase (FBA) as the physiological substrates of AtLSMT-L. These enzymes are involved in the assimilation of CO₂ through the Calvin cycle and in chloroplastic glycolysis. Trimethylation occurs at a highly conserved lysyl residue at the C-terminal end of FBAs. Finally, we found that this post-translational modification does not modify the kinetic properties of aldolases *in vitro*. To conclude, we discuss the evolution of LSMT-like enzymes protein substrate specificity and the possible involvement of protein methylation in the control of carbon metabolism in chloroplasts.

EXPERIMENTAL PROCEDURES

Materials—[methyl-³H]AdoMet (70–85 Ci·mmol⁻¹) was purchased from PerkinElmer Life Sciences. Chromatographic media were from GE Healthcare. Unless otherwise stated, other chemicals and reagents were from Sigma and of the highest purity available. AdoMet was further purified by ion exchange chromatography on CM-Sephadex C-25 (9).

Plant Growth Conditions—Wild-type and mutant *A. thaliana* (ecotype Columbia, Col-0) plants were grown on soil in a growth chamber (22 °C, 60% air humidity, light intensity of 120 μ mol of photons m⁻² s⁻¹, 16 h light/8 h dark). Seeds of the tDNA insertion lines SAIL_1156_C01 and SAIL_69_A09 were

obtained from the European Nottingham *Arabidopsis* Stock Centre (10).

Characterization of *Arabidopsis* Mutant Lines—*Arabidopsis* genomic DNA was isolated from a single leaf, and the insertions were checked by amplifying DNA fragments using gene-specific and tDNA-specific primers listed in supplemental Table 1 (11). Amplicons were sequenced to map the insertions. For RT-PCR and real time quantitative PCR (qPCR) experiments, total RNA was isolated from *Arabidopsis* leaves using the RNeasy plant mini extraction kit (Qiagen). RNA was treated with DNase I, and first strand cDNA was synthesized with the ThermoScript RT-PCR system (Invitrogen) using oligo(dT). Amplicons generated by PCR were analyzed by agarose gel electrophoresis. The real time qPCRs were carried out on a Rotor-Gene 3000 instrument (Qiagen) using SYBR Green JumpStart Taq ReadyMix (Sigma). Quantification of gene expression was performed using the comparative CT method with the Rotor-Gene 6000 series software. The ACTIN 7 gene (At5g09810) was used to normalize qPCR data. Primer sequences are available in supplemental Table 1.

Purification of Chloroplasts and Rubisco—Chloroplasts from 4-week-old *Arabidopsis* rosettes were purified on Percoll gradients as described previously (12). Intact chloroplasts were submitted to three freeze/thaw cycles to ensure complete lysis, and membranes (thylakoids plus envelope) were removed by centrifugation at 150,000 \times g for 30 min at 4 °C. Chloroplasts from pea and spinach leaves were purified and fractionated into stroma, thylakoids, and envelope as described previously (12, 13). Rubisco was purified from spinach chloroplasts as follows. Stromal proteins were precipitated with ammonium sulfate (50% saturation), desalted using a Sephadex G-25 PD-10 column equilibrated with 10 mM Hepes, pH 7.8, and 5% (v/v) glycerol, and applied onto a Q-Sepharose column equilibrated in the same buffer. Proteins were eluted using a KCl linear gradient, and fractions containing Rubisco were pooled and desalted.

Western Immunoblotting—Total soluble proteins from *Arabidopsis* leaves were extracted by grinding powdered samples in 50 mM Tris-HCl, pH 8.0, 1 mM dithiothreitol, 5% (v/v) glycerol, and a mixture of protease inhibitors (Roche Applied Science). Samples were centrifuged at 16,000 \times g for 20 min at 4 °C, and the supernatant used as a source of soluble proteins. Proteins were resolved by SDS-PAGE, electroblotted to nitrocellulose membrane, and probed using AtLSMT-L or FBA2 polyclonal antibodies produced in guinea pig or rabbit (Charles River Laboratories, France). Blots were also probed with rabbit polyclonal antibodies to trimethylated Lys (ab76118, Abcam). Protein quantification was achieved using the ECL Plus™ Western blotting detection reagents and a Typhoon 9400 scanner (Amersham Biosciences).

cDNA Cloning and Expression Constructs—Full-length cDNAs for AtLSMT-L (At1g14030), AtPPKMT1 (At5g14260), FBA2 (At4g38970), FBAC1 (At3g52930), and γ TMT (At1g64970) were obtained from the *Arabidopsis* Biological Resource Center (14). For FBA3 (At2g01140) and PsLSMT, cDNAs were obtained by PCR amplification of cDNA libraries prepared from *Arabidopsis* (Col-0) or pea (var. Douce Provence) seedlings, respectively. Total RNAs were extracted as described above and reverse-transcribed using oligo(dT).

Amplification of the full-length coding sequence for the cytosolic protein FBAC1 and the mature (devoid of transit peptide) sequences for chloroplastic proteins was done using the Phusion® high fidelity DNA polymerase (Finnzymes) and primers containing the appropriate restriction sites (supplemental Table 1) for cloning into pET expression vectors (Novagen). Mature AtLSMT-L, PsLSMT, and AtPPKMT1 were cloned in pET23d(+), resulting in fusion proteins with a C-terminal hexahistidine tag. Full-length or mature putative protein substrates of LSMTs were cloned in pET28b(+) to produce fusions with an N-terminal His₆ tag.

Production and Purification of Recombinant Proteins—*Escherichia coli* Rosetta-2 cells (Stratagene) harboring pET constructs were grown to log phase at 37 °C in Luria-Bertani medium containing the appropriate antibiotics. Isopropylthio-β-D-galactoside was added, and the cells were further grown for 16 h at 17 °C. Cells were collected by centrifugation (4,000 × g, 20 min), suspended in buffer A (50 mM Tris, pH 8.0, 0.5 M NaCl) containing 10 mM imidazole and a mixture of protease inhibitors, and then disrupted by sonication. The soluble protein extract was separated from cell debris by centrifugation at 30,000 × g for 15 min and applied onto a nickel-Sepharose column previously equilibrated with buffer A containing 10 mM imidazole. The procedure for affinity purification was then adapted for each His-tagged protein. After successive washes, recombinant proteins were eluted with buffer A containing 50–250 mM imidazole. Fractions containing the His-tagged proteins were pooled, desalted using Sephadex G-25 PD-10 columns equilibrated with 50 mM Tris, pH 8.0, 0.3 M NaCl, and 10% (v/v) glycerol, and concentrated by centrifugal ultrafiltration (Amicon Ultra, 10-kDa cutoff, Millipore). Using this procedure, the purity of recombinant AtLSMT-L, PsLSMT, AtPPKMT1, FBAC1, and γTMT was >95% as estimated by SDS-PAGE and Coomassie Blue staining. For FBA2 and FBA3, an additional chromatographic step was introduced to improve purity. Proteins from the nickel-Sepharose step were desalted in 20 mM KH₂PO₄/K₂HPO₄, pH 7.4, and 5% (v/v) glycerol, applied onto a Q-Sepharose column equilibrated with the same buffer, and eluted using a KCl linear gradient. Active fractions were pooled and concentrated as before.

Assay for Methyltransferases—The activity of PKMTs toward different substrates was determined essentially as described previously (15, 16). Assay mixtures contained phosphate-buffered saline, pH 7.8, 20 μM [methyl-³H]AdoMet, purified PKMT, and various amounts of the protein substrate in a final volume of 20 μL. Assays were conducted at 30 °C and optimized for linearity with time and enzyme concentrations. Substrate consumption was limited to <20%. When extended incubation was required (e.g. for stoichiometric methylation of a protein substrate), the assay was added with 20 nM S-adenosylhomocysteine hydrolase to avoid LSMT inhibition by S-adenosylhomocysteine (17). Reactions were terminated by the addition of 500 μL of trichloroacetic acid 10% (w/v) and 5 μL sodium deoxycholate 1% (w/v). Proteins were treated as described previously (15), and incorporated radioactivity was determined by either liquid scintillation or by phosphorimaging. For phosphorimage analyses, proteins were resolved by SDS-PAGE and transferred to ProBlott membranes (Applied Biosystems). Membranes

were stained with Coomassie Blue, dried, and exposed to a tritium storage phosphor screen (GE Healthcare) for 5–8 days before phosphorimage analysis using a Typhoon 9400 scanner (Amersham Biosciences). Kinetic parameters were calculated from fitted Michaelis-Menten curves by using Kaleidagraph (Synergy Software).

Assays for Fructose Bisphosphate Aldolase—The fructose 1,6-bisphosphate (FBP) cleavage activity of aldolase was assayed by following NADH oxidation at 340 nm in a coupled system (18). Assays (500 μL) were performed at 30 °C in 40 mM triethanolamine pH 7.5, 10 mM EDTA, 10 units of α-glycerol-phosphate dehydrogenase, 1 unit of triose phosphate isomerase, 0.2 mM NADH, 2 mM FBP, and various amounts of FBA. The condensation reaction of aldolase to form FBP from triose phosphate was measured using a discontinuous assay (19). First, FBA was incubated at 30 °C in a reaction mixture (100 μL) composed of 100 mM triethanolamine, pH 7.5, 10 mM EDTA, 12 mM DL-glyceraldehyde 3-phosphate, and 12 mM dihydroxyacetone phosphate. The reaction was stopped by heating samples at 90 °C for 4 min and then cooling on ice. Second, FBP produced was titrated by following NADP reduction at 340 nm in an assay (500 μL; 37 °C) containing 40 mM triethanolamine, pH 7.5, 0.5 mM EDTA, 15 mM MgCl₂, 50 mM KCl, 0.1 unit of FBP phosphatase, 2 units of phosphoglucose isomerase, 1 unit of glucose 6-phosphate dehydrogenase, and 1 mM NADP. For both the condensation and cleavage reactions, assays were adjusted to ensure linearity as a function of time and enzyme concentration.

Assays for Interaction of SET Domain Proteins with Rubisco—Wells of microtiter ELISA plates were coated with purified spinach Rubisco (34 μg) and incubated for 1 h at 25 °C with various amounts of PsLSMT, AtLSMT-L, or AtPPKMT1. Following incubation, plates were washed with Tris-buffered saline containing 0.05% (v/v) Tween 20 and incubated successively with primary antibodies against methyltransferases and secondary antibodies conjugated to horseradish peroxidase. Enzyme activity was revealed in the presence of H₂O₂ and 2,2'-azino-bis(3-ethylbenzothiazoline-6-sulfonic acid), and the absorbance was determined at 405 nm.

Mass Spectrometry Methods—In-gel protein digestion with trypsin was carried out essentially as described previously (20, 21) using a Freedom EVO150 robotic platform (TECAN). Briefly, protein bands were manually excised from the gels and washed in NH₄HCO₃ and CH₃CN solutions. After dehydration in pure CH₃CN, proteins were oxidized in 100 μL of 7% (v/v) H₂O₂ for 15 min in the dark. After washing and drying, proteins were digested overnight at 37 °C in 25 mM NH₄HCO₃ containing 150 ng of sequencing grade modified trypsin (Promega). Peptides were then extracted from gel pieces using three sequential steps (15 min each) in 30 μL of 50% (v/v) CH₃CN, 30 μL of 5% (v/v) formic acid, and 30 μL of pure CH₃CN. The pooled supernatants were dried under vacuum.

LC-MS/MS experiments were performed on a LTQ-Orbitrap (Velos or XL) hybrid mass spectrometer (Thermo Fisher Scientific) coupled to an Ultimate 3000 LC System (Dionex). Peptide mixtures were desalted on line using a reverse phase precolumn (Acclaim PepMap 100 C18, 5 μm bead size, 100 Å pore size, 5 mm × 300 μm, Dionex) and resolved on a C18

column (Acclaim PepMap 100 C18, 3 μ m bead size, 100 Å pore size, 15 cm \times 75 μ m, Dionex). Peptides were separated using a 60-min gradient with aqueous solvent A (2% (v/v) CH₃CN, 0.1% (v/v) HCOOH) and solvent B (20% (v/v) CH₃CN, 0.1% (v/v) HCOOH) developed as follows: 4–45% B in 50 min, 45–90% B in 10 min, 90% B for 5 min. The full scan mass spectra were measured from m/z 400 to 1,600. The LTQ-Orbitrap mass spectrometer was operated in the data-dependent mode. The activation type used was collision-induced dissociation with standard normalized collision energy set at 35%.

Peak lists were generated with the Mascot Distiller version 2.3.2 software (Matrix Science) from the LC-MS/MS raw data. Using the Mascot 2.3 search engine (Matrix Science), MS/MS spectra were searched against an updated compilation of the *A. thaliana* protein database provided by TAIR (nuclear, mitochondrial, and plastid genome; TAIR version 9.0; June 19, 2009; 33,518 entries) and a homemade list of contaminants frequently observed in proteomics analyses (21). Two missed trypsin cleavage were allowed, and trypsin/P was used as the enzyme (cleavage at the C terminus of Lys/Arg, unless followed by Pro). The mass tolerances were 10 ppm for precursor ions and 1.0 Da for fragment ions. The variable modifications allowed were acetyl (protein N termini), Met oxidation and dioxidation, cysteic acid, methyl (Lys, Arg), dimethyl (Lys, Arg), and trimethyl (Lys). Mascot search results were automatically filtered using the home-developed IRMa 1.30.2 software (22). The following parameters were applied: (i) the number of report hits was fixed automatically to retrieve proteins with a p value, as defined by Mascot, such as $p < 0.05$; (ii) only peptides ranked first and with an homology threshold such as the p value, as defined by Mascot, corresponding to $p < 0.05$, were kept. Every duplicated peptide sequence was conserved. Spectra of interest were checked manually to confirm sequence and modifications.

To determine the mass of intact proteins, samples were desalted on line on a protein trap (Zorbax 300SB-C8, 5 μ m, 5 \times 0.3 mm, Agilent Technologies) and analyzed on a 6210 LC-TOF mass spectrometer coupled to an ESI source (Agilent Technologies). These analyses were conducted at the mass spectrometry platform of the Institut de Biologie Structurale, Grenoble, France.

RESULTS

AtLSMT-L Is Dispensable for *Arabidopsis* Growth in Ambient Environmental Conditions—Among the SET domain-containing PKMTs found in the *Arabidopsis* genome, the product of the At1g14030 gene is the closest homolog of LSMT from pea. This protein, referred to as AtLSMT-L for *Arabidopsis* LSMT-like, shares 62% sequence identity (plus 15% conservative changes) with PsLSMT. Hence, both the N-terminal located catalytic SET domain and the C-terminal lobe that forms extensive contacts with the LS Rubisco substrate are highly conserved between both proteins (23). AtLSMT-L is a 482-residue and 54.6-kDa protein harboring a predicted chloroplastic transit peptide. To support this prediction, AtLSMT-L was identified in the proteome of chloroplasts purified from *Arabidopsis* rosette leaves (24, 25) and found exclusively in the soluble stromal subfraction of the organelles (21).

To gain insight into the function of AtLSMT-L, two independent *Arabidopsis* lines carrying tDNA insertions in the At1g14030 gene were identified and characterized (supplemental Fig. 1). In the *lsmt1* mutant (SAIL_1156_C01), the insertion interrupted the open reading frame in the third exon, 173 residues downstream from the start codon. RT-PCR and Western blot analysis showed that this line is a loss-of-function allele that lacks the At1g14030 transcript and AtLSMT-L protein (supplemental Fig. 1). In the *lsmt2* mutant (SAIL_69_A09), the tDNA was located in the 5'-untranslated region of the gene, 38 nucleotides upstream the start codon, and resulted in a 80% decrease of At1g14030 transcript abundance, as estimated by RT-qPCR (supplemental Fig. 1). The residual AtLSMT-L protein detected in *lsmt2* (about 30% of the wild-type level) confirmed that this mutant line is knocked down for At1g14030 expression.

When grown in soil under standard temperature (22 °C) and light regimes (120 μ mol of photons $m^{-2} s^{-1}$), the knock-out and knockdown *lsmt* mutants did not differ visually from the wild type. Thus, the expected changes induced by loss or reduction of AtLSMT-L in chloroplasts were not associated with growth phenotypes in ambient environmental conditions.

Rubisco Is Not Methylated in *Arabidopsis*—To characterize the biochemical properties of AtLSMT-L, the mature enzyme (devoid of its transit peptide) was produced in *E. coli* as a His-tagged protein and purified by immobilized metal affinity chromatography. A recombinant His-tagged PsLSMT identical to the one characterized previously (15) was also purified and used as a control for testing methyl group transfer from [methyl-³H]AdoMet into protein substrates. Intact chloroplasts were purified from wild-type *Arabidopsis*, pea, and spinach leaves, fractionated to obtain soluble stromal proteins, and used as substrates for *in vitro* methylation assays. Using PsLSMT, a significant incorporation of tritiated methyl groups was observed in LS Rubisco from spinach, but no signal could be detected using pea stroma (Fig. 1). This result was expected because LS Rubisco from pea is methylated at Lys-14 *in vivo*, and thus cannot be methylated *in vitro*, whereas natural Rubisco from spinach is not modified and behaves as a good substrate for recombinant PsLSMT (2). LS Rubisco from *Arabidopsis* was also capable of accepting methyl groups from [methyl-³H]AdoMet, although at a lower rate than the spinach protein (Fig. 1; 4 versus 20 nmol of methyl groups incorporated $min^{-1} mg^{-1}$ of recombinant PsLSMT at 30 °C). This result suggests that LS Rubisco is not methylated or not fully methylated at Lys-14 in *Arabidopsis*.

To verify whether the modification of *Arabidopsis* LS Rubisco by PsLSMT occurred at Lys-14, the *in vitro* methylation assay was done with unlabeled AdoMet. LS Rubisco was then excised from a SDS-PAGE, digested with trypsin, and submitted to LC-MS/MS using an LTQ-Orbitrap mass spectrometer. To identify Lys-methylated peptides, MS/MS spectra were searched for mass shifts corresponding to mono-, di-, and trimethylation of Lys residues (see under "Experimental Procedures"). Among the 43 peptides identified for LS Rubisco (sequence coverage 63%), none contained an unmodified Lys-14, but this residue was found trimethylated in two nonredundant overlapping peptides (ASVGFK¹⁴AGVK and

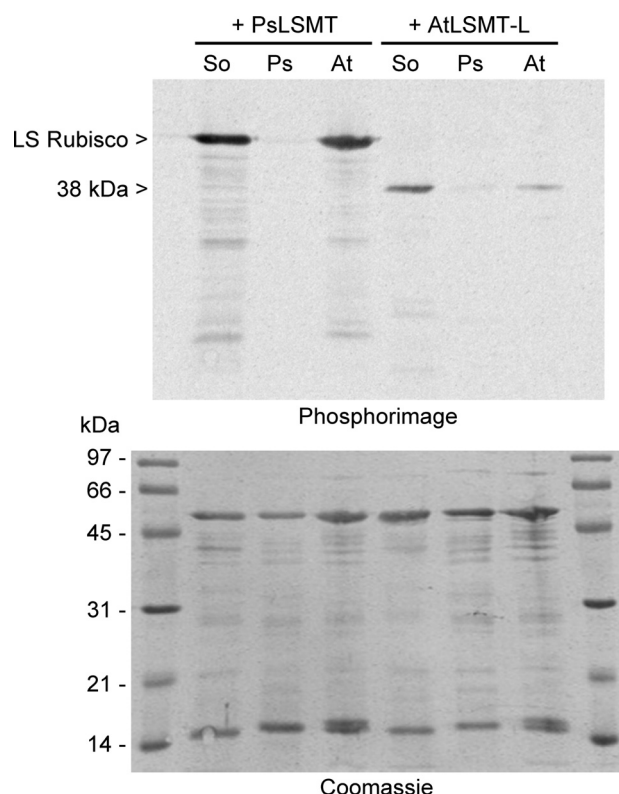


FIGURE 1. **Evidence for different protein substrate specificity between AtLSMT-L and PsLSMT.** Stroma was prepared from chloroplasts purified from spinach (*Spinacia oleracea*, So), pea (*Pisum sativum*, Ps) and *Arabidopsis* (At) leaves. Stromal fractions (20 μ g) were used as substrates for methylation assays with 20 μ M [$methyl-^3H$]AdoMet and recombinant AtLSMT-L (3 μ g) or PsLSMT (1 μ g). After incubation at 30 °C for 10 min (PsLSMT) or 30 min (AtLSMT-L), proteins were resolved by SDS-PAGE and transferred to ProBlott membranes. Membranes were stained with Coomassie Blue (lower panel) and used for phosphorimage analysis (upper panel).

ASVGFK¹⁴AGVKEYK, see supplemental Fig. 2 for MS/MS spectra). These peptides containing a trimethyl-Lys-14 were the most intense peptide ions, but monomethylated and dimethylated forms were also detected in less intense ions. When natural LS Rubisco from *Arabidopsis* was sequenced by LC-MS/MS (45 nonredundant peptides, sequence coverage 66%), no peptide covering Lys-14 was found. This result suggests an efficient tryptic cleavage of the N terminus of LS Rubisco into small peptides and thus no steric crowding due to a modification on lysyl residues (at position 8, 14, 18, or 21). These data strongly suggest that LS Rubisco is not naturally methylated (or poorly modified) at Lys-14 in wild-type *Arabidopsis* chloroplasts and behaves as a substrate of PsLSMT, as reported previously for LS Rubisco from spinach (2, 15).

Main Physiological Substrates of AtLSMT-L Are Fructose 1,6-Bisphosphate Aldolases—A similar approach was used to analyze the protein substrate specificity of recombinant AtLSMT-L. Methyl groups incorporation into stromal proteins was much lower than those recorded with PsLSMT (e.g. about 200 pmol \cdot min⁻¹ \cdot mg⁻¹ AtLSMT-L at 30 °C using spinach stroma). A phosphorimage of the protein methyl acceptor(s) indicated that the main soluble target of AtLSMT-L is not LS Rubisco but polypeptide(s) migrating at about 38 kDa in SDS-PAGE (Fig. 1). Different labeling intensities of this polypeptide(s) were observed in the various stromal fractions, likely due

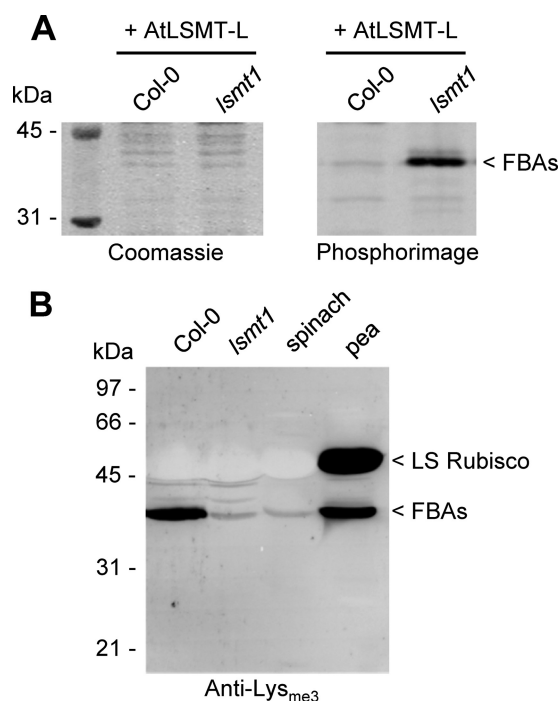


FIGURE 2. **Chloroplastic fructose 1,6-bisphosphate aldolases are substrates of AtLSMT-L in vivo.** A, chloroplastic FBAs (about 38 kDa) are hypomethylated *in vivo* in *lsmt1* and are methylatable *in vitro* by AtLSMT-L. Stroma was prepared from chloroplasts purified from wild-type (Col-0) and *lsmt1* plants. Stromal fractions (15 μ g) were incubated at 30 °C for 2 h with 20 μ M [$methyl-^3H$]AdoMet and recombinant AtLSMT-L (3 μ g). Proteins were treated as in Fig. 1 and used for phosphorimage analysis. B, probing chloroplastic soluble methyl proteins using antibodies specific to trimethyl-Lys. Stromal proteins (50 μ g) from *Arabidopsis* Col-0 and *lsmt1* lines, spinach, and pea were resolved by SDS-PAGE and probed using antibodies specific to trimethyl-Lys.

to different levels of methylation and/or abundance of the protein target(s) in *planta*.

To verify whether the 38-kDa protein(s) is the substrate of AtLSMT-L *in vivo*, we performed methylation assays using stromal proteins from the *lsmt1* mutant line. As shown in Fig. 2A, the incorporation of tritiated methyl groups is much higher in the 38-kDa polypeptide(s) from the knock-out *lsmt1* mutant than in the wild-type. These results indicate that the 38-kDa protein(s) is unmethylated (or poorly methylated) in *lsmt1*, thus suggesting strongly that it is the physiological substrate of AtLSMT-L. By comparing maximal methyl group incorporation into the 38-kDa protein(s) in Col-0 and *lsmt1* chloroplasts, we could calculate that this substrate is nearly fully methylated in the wild type ($97 \pm 2\%$, assuming an unmethylated status in *lsmt1* and using chloroplasts purified from leaves harvested 2–4 h after the onset of the light period).

With the aim of identifying the physiological protein target(s) of AtLSMT-L, stroma from Col-0 and *lsmt1* were resolved by SDS-PAGE; the 38-kDa bands were excised from the gel, and tryptic peptides were analyzed by LC-MS/MS. In the Col-0 sample, we identified three peptides bearing a trimethyl-Lys residue (Table 1 and supplemental Fig. 3 for MS/MS spectra). These peptides belong to isoforms of chloroplastic fructose 1,6-bisphosphate aldolase (FBA; EC 4.1.2.13), a 38-kDa protein involved in carbon metabolism. According to the TAIR database, the following nomenclature was used for these proteins: FBA1 (At2g21330), FBA2 (At4g38970), and

TABLE 1

Tryptic peptides covering the C terminus of chloroplastic FBA isoforms in the wild-type and *lsmt1* genetic backgrounds

Stromal fractions from wild-type (Col-0), *lsmt1*, and *lsmt1* methylated *in vitro* with recombinant AtLSMT-L were resolved by SDS-PAGE, and tryptic peptides were generated from the excised 38-kDa protein bands. MS/MS spectra were obtained using a LTQ-Orbitrap mass spectrometer, and data were searched for methyl peptides (see under "Experimental Procedures"). Lysyl residues corresponding to positions 395/394 for FBA1/FBA2 and 387 for FBA3 are underlined in peptide sequences. Only the most intense peptide ions covering the C terminus of chloroplastic FBAs are shown. In Col-0, less intense peptide ions are detected with monomethyl and dimethyl forms of Lys-395/394 in FBA1/FBA2. These peptides account for 5% of the sum of intensity of parent ions bearing the lysyl residue of interest (*i.e.* 95% are trimethylated). In the *lsmt1* + AtLSMT-L sample, peptides with unmodified Lys-395/394 in FBA1/FBA2 are detected and account for 4% of the sum of ions intensity. MS/MS spectra are available in supplemental Fig. 3.

Stromal sample	Peptide	Sequence	Modification	Mass measured	Mass calculated	Δ (ppm)	Mascot score	
FBA1 (At2g21330)/ FBA2 (At4g38970) <i>lsmt1</i> <i>lsmt1</i> + AtLSMT-L	Col-0	390–399/389–398	EGMFV <u>K</u> GYTY	K395/394 _{4me3}	1235.592	1235.590	2.03	44.25
		379–399/378–398	YTGEGESEEAKEGMFV <u>K</u> GYTY	K395/394 _{me3}	2416.082	2416.078	1.83	88.16
	<i>lsmt1</i>	379–395/378–394	YTGEGESEEAKEGMFV <u>K</u>		1889.828	1889.835	−4.00	107.76
		379–398/378–398	YTGEGESEEAKEGMFV <u>K</u> GYTY		2374.028	2374.031	−1.21	95.98
		370–395/369–394	ANSLAQLGKYTGEGESEEAKEGMFV <u>K</u>		2772.314	2772.328	−4.76	134.13
	<i>lsmt1</i> + AtLSMT-L	379–395/378–394	YTGEGESEEAKEGMFV <u>K</u>	K395/394 _{me3}	1931.868	1931.882	−7.25	80.81
		379–399/378–398	YTGEGESEEAKEGMFV <u>K</u> GYTY	K395/394 _{me3}	2416.075	2416.078	−1.40	84.21
	FBA3 (At2g01140) <i>lsmt1</i> <i>lsmt1</i> + AtLSMT-L	Col-0	383–391	GMFV <u>K</u> GYTY	K387 _{me3}	1106.547	1106.547	0.03
<i>lsmt1</i>		371–387	YSAEGENEDAKKGMFV <u>K</u>		1901.872	1901.883	−5.69	45.94
		383–391	GMFV <u>K</u> GYTY	K387 _{me3}	1106.545	1106.547	m1.76	45.96

FBA3 (At2g01140). Isoforms 1 and 2 share 93% identity over the complete protein sequence, and the third isoform displays 79% identity with FBA1/FBA2. Trimethylation takes place close to the C terminus of the proteins, at Lys-395/394 for FBA1/FBA2, which share the same peptide, and at Lys-387 for FBA3 (Table 1 and supplemental Fig. 3). Peptides covering the C terminus of FBA isoforms were also identified in the 38-kDa band from the *lsmt1* mutant, but none was methylated at the Lys residues identified above (Table 1). A stromal fraction from *lsmt1* was also methylated *in vitro* with recombinant AtLSMT-L prior to electrophoresis and sequencing. Peptides bearing trimethyl-Lys residues at the C termini of the three FBA isoforms were identified (Table 1), thus indicating that the *in vitro* methylation assay with recombinant AtLSMT-L did not introduce artifacts in the incorporation of methyl groups into FBA proteins. Together, these data indicate that chloroplastic FBA isoforms are the physiological targets of AtLSMT-L.

To verify the methylation status of FBAs *in vivo*, we performed Western blot analysis using antibodies to trimethyl-Lys and stromal fractions from wild-type and *lsmt1* *Arabidopsis* chloroplasts, as well as pea and spinach. As shown in Fig. 2B, LS Rubisco was labeled only in pea, confirming that the enzyme from *Arabidopsis* is not naturally trimethylated at Lys-14, as in spinach. Bands of high intensity migrating at about 38 kDa were detected in pea and Col-0 extracts and most likely correspond to trimethylated FBAs. In the *lsmt1* genetic background, the signal at 38 kDa was almost completely abolished, thereby confirming that FBAs are the major physiological substrates of AtLSMT-L. It should be noted that faint bands are detected by the antibodies in the Col-0, *lsmt1*, and spinach fractions, suggesting the existence of additional low abundant stromal proteins harboring trimethyl-Lys residues.

To confirm the identification of FBAs as new chloroplastic methyl proteins, we overexpressed the mature coding sequence (without transit peptide) of the *Arabidopsis* isoforms FBA2 and FBA3 in *E. coli*. Because FBA1 and FBA2 share 93% sequence identity and identical C termini, FBA2 was used as a prototype for both isoforms. The wild-type FBA2 and FBA3 proteins and a FBA2 mutant bearing a substitution of Lys-394 by Ala

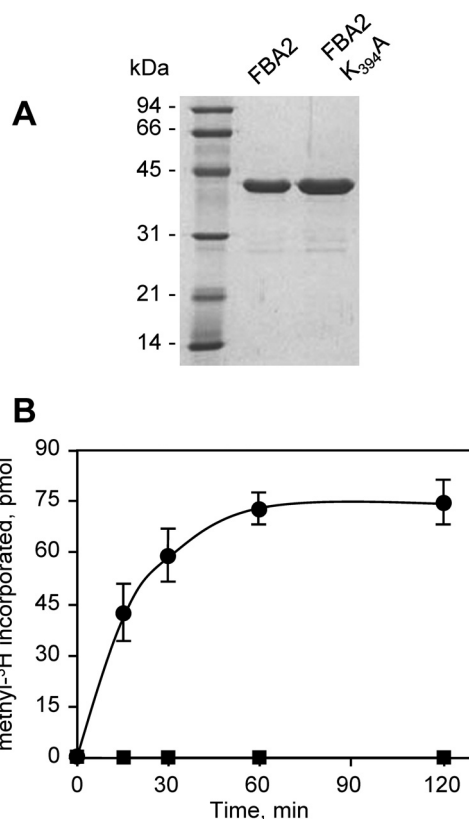


FIGURE 3. Stoichiometric trimethylation of recombinant FBA2 at Lys-394 by AtLSMT-L. A, documentation on purification of recombinant FBA2 and FBA2K394A. Purified proteins (4–6 μ g) were analyzed by SDS-PAGE and stained with Coomassie Blue. B, recombinant FBA2 proteins (25 pmol per time point) were incubated for the indicated time at 30 °C with 20 μ M [methyl- 3 H]AdoMet and recombinant AtLSMT-L (2 μ g). Methyl- 3 H incorporated into FBA2 (●) and FBA2K394A (■) was counted by liquid scintillation. Values are means \pm S.D. of three determinations.

(FBA2K394A) were purified as His-tagged fusion proteins (Fig. 3A). The tag was inserted at the N terminus of the recombinant proteins to avoid interference with the methylation site located close to the C terminus. Pure proteins were used for *in vitro* methylation assays using recombinant AtLSMT-L. As shown in

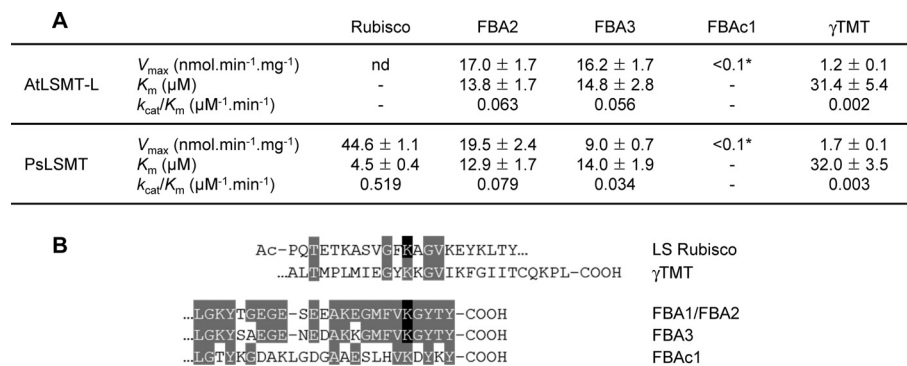


FIGURE 4. Kinetic parameters of AtLSMT-L and PsLSMT toward different protein substrates. A, values are means ± S.D. as estimated by nonlinear square refinement of the kinetic data. nd, not detected in our experimental conditions. *, specific activities determined with 25 μM FBAc1; kinetic parameters could not be determined with confidence for this substrate. B, sequences of the region embedding the lysyl methylation sites in the different protein substrates. Because of low similarities, alignments have been done using two sets of Arabidopsis proteins, LS Rubisco and γ TMT on the one hand, FBA isoforms on the other hand. Identical residues in at least two sequences are shaded in gray, and proven methylated Lys residues are in black.

Fig. 3B, incorporation of methyl groups into FBA2 was significant, and extended incubation periods (>60 min in our conditions) resulted in a stoichiometric trimethylation of the protein (75 pmol of methyl incorporated into 25 pmol of FBA2; Fig. 3B). A similar result was obtained with FBA3 (data not shown). When the assay was done with the FBA2K394A protein, no incorporation of tritiated methyl group was observed (Fig. 3B). These data clearly show that FBA proteins are trimethylated by AtLSMT-L at a unique Lys residue present in their C termini.

Comparison of Kinetic Properties of AtLSMT-L and PsLSMT toward Various Substrates—To gain insight into the protein substrate specificity of AtLSMT-L and PsLSMT, we analyzed the kinetic parameters of both enzymes using different purified protein targets. Rubisco was purified from spinach stroma by ion exchange chromatography. This source of unmethylated enzyme was shown to be representative of the interaction that occurs between LSMT and Rubisco (23). In addition to FBA2 and FBA3, two candidate protein substrates from Arabidopsis were also produced in E. coli as fusions with His tags at their N termini, i.e. at the opposite end of the hypothetical methylation sites. First, the full-length sequence of an Arabidopsis cytosolic isoform of aldolase (FBAc1, At3g52930) was expressed to test whether a protein that does not colocalize with AtLSMT-L in chloroplasts but possesses a conserved Lys residue in the C-terminal region could behave as a substrate. Second, we produced the mature coding sequence of γ TMT from Arabidopsis, a chloroplastic enzyme involved in tocopherols synthesis. Indeed, recombinant γ TMT from Perilla frutescens was previously shown to be an alternative substrate of PsLSMT in vitro (8). Purified recombinant proteins were analyzed by mass spectrometry to ensure that the potential substrates, and in particular their methylation sites, have not been damaged during protein isolation.

The kinetic parameters determined for AtLSMT-L and PsLSMT using these different substrates are summarized in Fig. 4A. First, the V_{\max} and K_m values determined for PsLSMT and spinach Rubisco are similar to those previously reported (15), thus demonstrating that the two batches of enzyme and in vitro assay conditions are comparable. Also, we confirmed our previous results obtained with stroma from spinach (Fig. 1) by showing that AtLSMT-L is unable to use purified unmethylated

Rubisco as a substrate. Chloroplastic FBAs behaved as good substrates of AtLSMT-L (K_m of about 14 μM and V_{\max} of about 17 nmol min⁻¹ mg⁻¹), whereas methylation rates with the cytosolic isoform were very low. A similar kinetic behavior was observed for PsLSMT, which utilizes FBA2 and FBA3 as alternative substrates to Rubisco, but not the cytosolic protein FBAc1. All the FBA proteins have a relatively conserved C-terminal sequence embedding the methylatable Lys residue (Fig. 4B), and the differences observed are unlikely associated with protein degradation or misfolding because the three recombinant FBAs are active and have the expected molecular masses, as determined by mass spectrometry (data not shown). Recombinant γ TMT was a poor substrate for both LSMT-like enzymes, with k_{cat}/K_m values 20 to 30 times lower than with FBA2 as a substrate. In the case of PsLSMT, the specificity constant was 170 times lower with γ TMT than with Rubisco.

AtLSMT-L Interacts with Rubisco in a Catalytically Unproductive Way—The inability of AtLSMT-L to methylate LS Rubisco both in vitro and in vivo could result from the incapacity of the enzyme to bind Rubisco or from an interaction incompatible with methyl group transfer from AdoMet to Lys-14. To discriminate between these two hypotheses, we developed an ELISA to analyze the interaction between chloroplastic PKMTs and unmethylated Rubisco (see “Experimental Procedures”). As shown in Fig. 5A, the binding of PsLSMT and AtLSMT-L to immobilized spinach Rubisco is concentration-dependent and saturable. Estimated dissociation constant values are comparable for both methyltransferases (0.87 ± 0.26 and 1.11 ± 0.33 μM for PsLSMT and AtLSMT-L, respectively). To control the specificity of AtLSMT-L interaction with Rubisco, ELISA was done with another chloroplastic SET domain protein from Arabidopsis, encoded by the At5g14260 gene. This protein, referred to as AtPPKMT1 for plastid PKMT, is unable to methylate Rubisco or chloroplastic aldolases in vitro.³ No significant binding of AtPPKMT1 to Rubisco was observed (Fig. 5A). To confirm these data, we tested whether AtLSMT-L could compete with PsLSMT for interaction with Rubisco. To this aim, purified Rubisco was preincubated with various amounts of

³ S. Ravel and C. Alban, unpublished data.

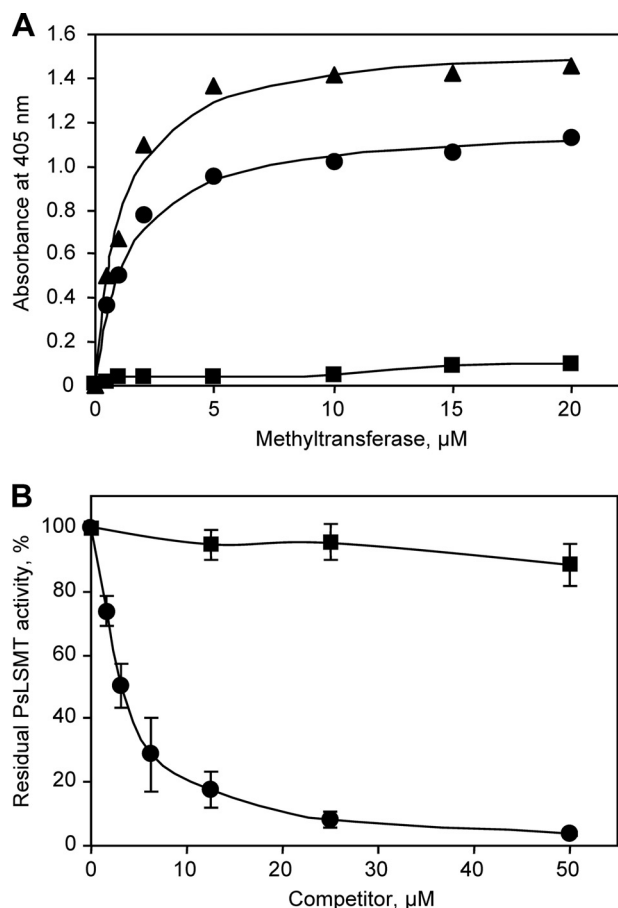


FIGURE 5. Interaction of AtLSMT-L with unmethylated Rubisco. A, interaction of AtLSMT-L and PsLSMT with immobilized spinach Rubisco. Rubisco coated into wells of microtitration plates was incubated at 25 °C for 60 min with increasing amounts of pure recombinant PsLSMT (▲), AtLSMT-L (●), or AtPPKMT1 (■). AtPPKMT1 is a chloroplastic SET domain protein with no activity using Rubisco or FBAs as substrates.³ The fraction of bound enzymes was determined using antibodies against AtLSMT-L (for AtLSMT-L and PsLSMT) or AtPPKMT1 followed by measurements of secondary antibody-linked peroxidase activity at 405 nm. Curves are representative of data from three independent repeats and were fitted to a hyperbola for PsLSMT and AtLSMT-L. B, competition of AtLSMT-L with PsLSMT for interaction with unmethylated Rubisco. Spinach Rubisco (1.5 μM) was incubated at 25 °C for 60 min with various concentrations of purified recombinant AtLSMT-L (●) or AtPPKMT1 (■). Following incubation, PsLSMT activity was determined at 30 °C with 20 μM [methyl-³H]AdoMet and 0.5 μM recombinant PsLSMT. Values are means \pm S.D. of three determinations. Preincubation of Rubisco with bovine γ -globulins (up to 80 μM) did not affect PsLSMT activity.

AtLSMT-L and further incubated with PsLSMT and [methyl-³H]AdoMet. Results shown in Fig. 5B indicate that AtLSMT-L is able to compete with PsLSMT for interaction with Rubisco. Again, the interaction of AtLSMT-L is specific because PsLSMT activity is not impaired by preincubation with AtPPKMT1 or unrelated proteins (bovine γ -globulins). Together, these data show that AtLSMT-L interacts with unmethylated Rubisco but that the complex is catalytically inefficient.

Biochemical Properties of Chloroplastic FBAs Are Not Affected by Methylation of the C-terminal Domain—To determine whether trimethylation of chloroplastic FBAs modifies the biochemical properties of the enzyme, we compared the activities of the unmodified and methylated proteins. Chloroplastic FBA catalyzes several important reactions in carbon

metabolism. First, the aldolase is involved in two reactions of the Calvin cycle, the reversible aldol condensation of dihydroxyacetone phosphate and either D-glyceraldehyde 3-phosphate or erythrose 4-phosphate to yield FBP or sedoheptulose 1,7-bisphosphate. Second, the hydrolysis of FBP into triose phosphate is a key step in chloroplastic glycolysis. The FBP cleavage reaction and the reverse condensation process were determined spectrophotometrically using recombinant FBA2 and FBA3, unmethylated or stoichiometrically trimethylated with AtLSMT-L (see Fig. 3B). Specific activities of the two unmodified enzymes are comparable, with a condensation activity about 2.8-fold higher than the cleavage reaction (Fig. 6A). Also, a substitution of the methylable lysyl residue by an Ala (FBA2K394A mutant) has no effect on enzyme activity. These properties have been previously reported in a study dedicated to the functional role of the C terminus of recombinant cytosolic maize aldolase (26). Stoichiometric trimethylation of FBA2 and FBA3 in the C-terminal region did not alter the specific activity of the enzyme in both directions (Fig. 6A). Also, the kinetic parameters for FBP cleavage are similar for the unmodified or trimethylated enzymes and for the FBA2K394A mutant, with V_{max} and K_m values for FBP of about 13–15 $\mu\text{mol}\cdot\text{min}^{-1}\cdot\text{mg}^{-1}$ at 30 °C and 35–45 μM , respectively. These results suggest that methylation of chloroplastic aldolases does not modify the catalytic properties of the enzymes. However, data obtained with purified recombinant proteins may not reflect the physiological status of the enzymes, which can be controlled, for example, by other post-translational modification(s). Thus, the FBP cleavage and triose phosphate condensation reactions were measured using stroma from wild-type and *lsmt1* chloroplasts. Both activities are similar in the two types of purified organelles (Fig. 6A), and Western blot analysis indicates a similar amount of the enzyme in both samples (Fig. 6B). Together, these data demonstrate that trimethylation of chloroplastic FBAs in a physiological context does not affect the kinetic properties or stability of the enzyme.

Plant FBAs belong to the class I aldolases and behave as tetramers (18). To test whether trimethylation at the C terminus of FBA can influence its oligomerization state, we analyzed the unmodified and methylated enzymes by native PAGE. This was done using pure recombinant FBA2 or stroma from Col-0 and *lsmt1* followed by staining with Coomassie Blue or immunodetection, respectively. As shown in Fig. 6B, both the native or recombinant chloroplastic aldolases are tetramers, and methylation does not affect the oligomerization of the enzyme.

DISCUSSION

In this work, we report the identification of chloroplastic isoforms of FBA as the physiological soluble substrates of the LSMT-like enzyme in *Arabidopsis*. Contrary to PsLSMT, AtLSMT-L is unable to use purified unmethylated spinach Rubisco as a substrate. Moreover, we showed that LS Rubisco is not naturally methylated at Lys-14 in *Arabidopsis*, thus indicating that neither AtLSMT-L nor another chloroplastic PKMT is able to modify this residue *in vivo*. LS Rubisco from *Arabidopsis* was recently shown to be acetylated at multiple lysyl residues, including Lys-14 (27). Because this protein can be methylated *in*

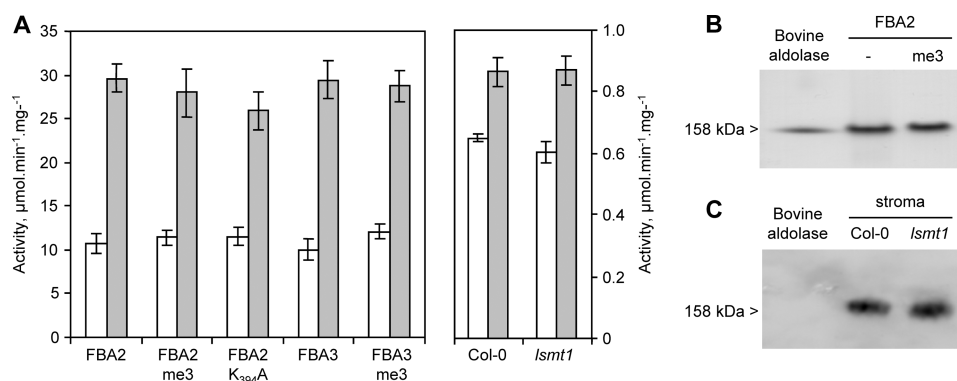


FIGURE 6. Unmethylated and methylated chloroplastic FBAs display similar kinetic properties and oligomeric states. A, cleavage (white bars) and condensation (gray bars) activities catalyzed by aldolase were determined for the recombinant FBA2 and FBA3 proteins (left panel), and for stroma prepared from Col-0 and *lsmt1* chloroplasts (right panel). The wild-type FBA2 and FBA3 enzymes were analyzed under both the unmethylated and stoichiometrically trimethylated (me3) states. Values for the FBA2K394A protein were similar with or without prolonged incubation with AtLSMT-L and AdoMet. Values are means \pm S.D. for at least three measurements of activities in both directions using different batches of enzyme. B and C, electrophoretic behavior of recombinant and natural chloroplastic FBAs under unmodified and methylated forms in native PAGE. Recombinant FBA2 (4 μ g) under unmodified (–) or stoichiometrically trimethylated (me3) states was analyzed by native PAGE and stained with Coomassie Blue (B). Stroma (6 μ g) from Col-0 and *lsmt1* was resolved by native PAGE, transferred to nitrocellulose, and analyzed using antibodies against FBA2 (C). Bovine aldolase (158 kDa) was used as a molecular mass standard.

in vitro by PsLSMT at this position (Fig. 1 and supplemental Fig. 2), one can conclude that Lys-14 in LS Rubisco from *Arabidopsis* is either unmodified or partially acetylated *in vivo* but is not trimethylated.

Together, our results indicate that LSMT-like enzymes from *Arabidopsis* and pea display different substrate specificity with respect to LS Rubisco and almost similar properties regarding other substrate targets. Thus, both AtLSMT-L and PsLSMT accept chloroplastic FBAs as substrates but not a cytosolic aldolase with a conserved lysyl residue in the C terminus. Also, recombinant γ TMT from *Arabidopsis* is a poor substrate for both LSMT-like enzymes, with a specificity constant (k_{cat}/K_m) 1 or 2 orders of magnitude lower than with FBAs or Rubisco as substrates (Fig. 4). Thus, the significance of γ TMT methylation *in vivo* is still questionable. Finally, there is no difference in the product specificity of the two protein methyltransferases, both transferring three methyl groups to the lysyl acceptor.

To gain insight into the substrate preference of plant LSMT-like proteins, we showed that the *Arabidopsis* enzyme is able to interact with unmethylated Rubisco with an estimated dissociation constant comparable with that of PsLSMT (Fig. 5). These results suggest strongly that the inability of AtLSMT-L to methylate Rubisco is due to a catalytic defect rather than a lack of interaction between partners. The atomic model of the complex between Rubisco and PsLSMT supports this view because the C-terminal lobe and the SET domain that confer specificity of PsLSMT for Rubisco recognition are highly conserved in LSMT-like proteins, including AtLSMT-L (23). Also, the unmethylated status of Rubisco in *Arabidopsis* and other species like spinach or wheat does not reflect sequence divergence of LS around the Lys-14 methylation site (see supplemental Fig. 4) or the residues mediating the interaction with the methyltransferase (23). The structure of the active site of PsLSMT indicated that the LS Rubisco and AdoMet substrates bind to separate clefts connected by a pore large enough to accommodate the transfer of methyl groups to Lys-14 (16). All the residues involved in AdoMet binding and all but one residue involved in the Lys-14-binding site are conserved between PsLSMT and AtLSMT-L (His-252 in PsLSMT is substituted by

a Tyr residue in AtLSMT-L). We hypothesize therefore that a limited number of amino acid substitutions associated with subtle structural differences of the SET domain and regions immediately adjacent to the core catalytic domain are responsible for an unfavorable conformation of the ϵ -amine of the substrate in the Lys channel, leading to an inhibition in methyl group transfer to Lys-14 of Rubisco by AtLSMT-L.

Trimethylation of aldolases by LSMT-like enzymes occurs close to the C terminus, in a region that is highly conserved in chloroplastic isoenzymes from various plant species. The methylation motif in chloroplastic FBAs, (Met/Leu)-Phe-Val-Lys-(Gly/Asn)-Tyr-(Ser/Val/Thr)-Tyr-COOH, shares limited similarity with the consensus sequence flanking the LS Rubisco Lys-14 methylation site previously determined for PsLSMT (Gly/Ser)-(Phe/Tyr)-Lys-(Ala/Lys/Arg)-(Gly/Ser) (Fig. 4B and supplemental Fig. 4) (8). Given that PsLSMT is able to trimethylate efficiently lysyl residues embedded in these two motifs (Fig. 4), it is obvious that the primary polypeptide sequence is not sufficient to predict protein substrates for this methyltransferase and possibly other LSMT-like enzymes. However, the N terminus of LS Rubisco and the C terminus of chloroplastic aldolases share common features that could be important determinants for substrate specificity. Indeed, the Lys-14 residue on LS Rubisco is located in the random coil and solvent-accessible N-terminal region, a situation that is analogous to the methylation sites in the N-terminal tails of histone H3 and H4 (28). The three-dimensional structures of tetrameric type I FBAs from eukaryotes have been solved, and the C terminus was found exposed to the solvent and relatively flexible (e.g. Ref. 29). The criteria of solvent accessibility and flexibility seem essential for recognition and binding of the protein substrate in the appropriate binding cleft of the PKMT, but they are not sufficient for a productive binding, *i.e.* followed by methyl group transfer, because (i) AtLSMT-L binds to but does not methylate Rubisco, and (ii) a cytosolic FBA with a solvent-accessible and flexible C-terminal domain behaves as a very poor substrate for AtLSMT-L and PsLSMT (Fig. 4). Thus, the polypeptide substrate specificity of LSMT homologs obeys complex and yet incompletely understood rules, and it is likely

that alternative substrates could be identified in the future, particularly in species like spinach where neither Rubisco nor FBAs are trimethylated *in vivo* (Fig. 2B).

Chloroplastic aldolases are shared between the Calvin cycle, where they contribute to the regeneration of the CO₂ acceptor molecule ribulose 1,5-bisphosphate, and the plastidic glycolysis, which provides precursors for amino acid and fatty acid synthesis. It has been shown previously that these reversible enzymes have impact on carbon flux through the Calvin cycle and that the acclimation of photosynthesis to changing environmental conditions (light and CO₂ regimes) includes and requires changes in plastidic aldolase activity (30–33). Thus, the identification of FBAs as methyl proteins *in vivo*, at least in *Arabidopsis* and pea (Fig. 2B), suggests that methylation may have a role in carbon metabolism in plastids. The lysyl methylation site is located in the C terminus of the enzyme, a region that is known to modulate the catalytic activity of cytosolic aldolases (26). However, our results indicate that stoichiometric trimethylation does not modify the catalytic properties of chloroplastic FBAs *in vitro*, for the glycolytic (cleavage) and photosynthetic (condensation) reactions (Fig. 6A). It is therefore possible that the functional significance of plastidic aldolase methylation lies with regulatory mechanisms involving protein-protein interactions, as hypothesized for Rubisco methylation (2).

It is generally assumed that methylation of Lys residues modifies intra- or intermolecular interactions and provides regulatory binding surfaces for protein partners (3). Evidence that enzymes of the Calvin cycle, including aldolase, are organized in supramolecular complexes with different compositions comes from a number of studies (for a review, see Ref. 34). Notably, FBA from the green algae *Chlamydomonas reinhardtii* was shown to associate tightly with a ternary complex composed of glyceraldehyde-3-phosphate dehydrogenase, phosphoribulokinase, and the regulatory protein CP12 (19). The interaction is transient, and in the presence of the ternary complex, the FBP cleavage activity was increased by 50%, whereas the triose phosphate condensation activity was not affected. Therefore, it is tempting to postulate that the methylation state of aldolases may influence the recruitment of partners to favor photosynthesis or glycolysis depending on the environmental conditions (e.g. light or nutrient availability) and/or metabolic demands (carbon partitioning between starch, amino acids, or fatty acid synthesis). Noteworthy, aldolases together with numerous enzymes involved in chloroplastic carbon metabolism were found to be phosphorylated and/or acetylated (27, 32, 35). Therefore, there may be a complex interplay of different post-translational modifications to regulate *in vivo* the dual function of aldolases in the Calvin cycle and glycolytic pathway. Cracking the “FBA code,” with reference to the histone code, is an important challenge because plastidic aldolases might be targets for increasing photosynthetic carbon flux to improve crop yield (36).

Acknowledgment—We thank Dr. Fabrice Rébeillé for helpful discussions.

REFERENCES

- Ng, D. W., Wang, T., Chandrasekharan, M. B., Aramayo, R., Kertbundit, S., and Hall, T. C. (2007) Plant SET domain-containing proteins. Structure, function, and regulation. *Biochim. Biophys. Acta* **1769**, 316–329
- Dirk, L. M., Trievel, R. C., and Houtz, R. L. (2006) in *The Enzymes* (Tamaio, F., and Clarke, S., eds) pp. 179–228, Elsevier Academic Press, Burlington, MA
- Huang, J., and Berger, S. L. (2008) The emerging field of dynamic lysine methylation of non-histone proteins. *Curr. Opin. Genet. Dev.* **18**, 152–158
- Aquea, F., Vega, A., Timmermann, T., Poupin, M. J., and Arce-Johnson, P. (2011) Genome-wide analysis of the SET DOMAIN GROUP family in grapevine. *Plant Cell Rep.* **30**, 1087–1097
- Huang, Y., Liu, C., Shen, W. H., and Ruan, Y. (2011) Phylogenetic analysis and classification of the *Brassica rapa* SET domain protein family. *BMC Plant Biol.* **11**, 175
- Houtz, R. L., Magnani, R., Nayak, N. R., and Dirk, L. M. (2008) Co- and post-translational modifications in Rubisco. Unanswered questions. *J. Exp. Bot.* **59**, 1635–1645
- Houtz, R. L., Poneleit, L., Jones, S. B., Royer, M., and Stults, J. T. (1992) Post-translational modifications in the amino-terminal region of the large subunit of Ribulose-1,5-bisphosphate carboxylase/oxygenase from several plant species. *Plant Physiol.* **98**, 1170–1174
- Magnani, R., Nayak, N. R., Mazarei, M., Dirk, L. M., and Houtz, R. L. (2007) Polypeptide substrate specificity of PsLSMT. A set domain protein methyltransferase. *J. Biol. Chem.* **282**, 27857–27864
- Curien, G., Ravel, S., and Dumas, R. (2003) A kinetic model of the branch point between the methionine and threonine biosynthesis pathways in *Arabidopsis thaliana*. *Eur. J. Biochem.* **270**, 4615–4627
- Alonso, J. M., Stepanova, A. N., Leisse, T. J., Kim, C. J., Chen, H., Shinn, P., Stevenson, D. K., Zimmerman, J., Barajas, P., Cheuk, R., Gadrinab, C., Heller, C., Jeske, A., Koesema, E., Meyers, C. C., Parker, H., Prednis, L., Ansari, Y., Choy, N., Deen, H., Geraht, M., Hazari, N., Hom, E., Karnes, M., Mulholland, C., Ndubaku, R., Schmidt, I., Guzman, P., Aguilar-Henonin, L., Schmid, M., Weigel, D., Carter, D. E., Marchand, T., Risseuw, E., Brogden, D., Zeko, A., Crosby, W. L., Berry, C. C., and Ecker, J. R. (2003) Genome-wide insertional mutagenesis of *Arabidopsis thaliana*. *Science* **301**, 653–657
- Edwards, K., Johnstone, C., and Thompson, C. (1991) A simple and rapid method for the preparation of plant genomic DNA for PCR analysis. *Nucleic Acids Res.* **19**, 1349
- Salvi, D., Rolland, N., Joyard, J., and Ferro, M. (2008) Purification and proteomic analysis of chloroplasts and their suborganellar compartments. *Methods Mol. Biol.* **432**, 19–36
- Ravel, S., Cherest, H., Jabrin, S., Grunwald, D., Surdin-Kerjan, Y., Douce, R., and Rébeillé, F. (2001) Tetrahydrofolate biosynthesis in plants. Molecular and functional characterization of dihydrofolate synthetase and three isoforms of folylpolyglutamate synthetase in *Arabidopsis thaliana*. *Proc. Natl. Acad. Sci. U.S.A.* **98**, 15360–15365
- Yamada, K., Lim, J., Dale, J. M., Chen, H., Shinn, P., Palm, C. J., Southwick, A. M., Wu, H. C., Kim, C., Nguyen, M., Pham, P., Cheuk, R., Karlin-Newmann, G., Liu, S. X., Lam, B., Sakano, H., Wu, T., Yu, G., Miranda, M., Quach, H. L., Tripp, M., Chang, C. H., Lee, J. M., Toriumi, M., Chan, M. M., Tang, C. C., Onodera, C. S., Deng, J. M., Akiyama, K., Ansari, Y., Arakawa, T., Banh, J., Banno, F., Bowser, L., Brooks, S., Carninci, P., Chao, Q., Choy, N., Enju, A., Goldsmith, A. D., Gurjal, M., Hansen, N. F., Hayashizaki, Y., Johnson-Hopson, C., Hsuan, V. W., Iida, K., Karnes, M., Khan, S., Koesema, E., Ishida, J., Jiang, P. X., Jones, T., Kawai, J., Kamiya, A., Meyers, C., Nakajima, M., Narusaka, M., Seki, M., Sakurai, T., Satou, M., Tamse, R., Vaysberg, M., Wallender, E. K., Wong, C., Yamamura, Y., Yuan, S., Shinozaki, K., Davis, R. W., Theologis, A., and Ecker, J. R. (2003) Empirical analysis of transcriptional activity in the *Arabidopsis* genome. *Science* **302**, 842–846
- Zheng, Q., Simel, E. J., Klein, P. E., Royer, M. T., and Houtz, R. L. (1998) Expression, purification, and characterization of recombinant ribulose-1,5-bisphosphate carboxylase/oxygenase large subunit ϵ -N-methyltransferase. *Protein Expr. Purif.* **14**, 104–112
- Trievel, R. C., Beach, B. M., Dirk, L. M., Houtz, R. L., and Hurley, J. H.

- (2002) Structure and catalytic mechanism of a SET domain protein methyltransferase. *Cell* **111**, 91–103
17. Suh-Lailam, B. B., and Hevel, J. M. (2010) A fast and efficient method for quantitative measurement of S-adenosyl-L-methionine-dependent methyltransferase activity with protein substrates. *Anal. Biochem.* **398**, 218–224
18. Horecker, B. L. (1975) Fructose biphosphate aldolase from spinach. *Methods Enzymol.* **42**, 234–239
19. Eroles, J., Avilan, L., Lebreton, S., and Gontero, B. (2008) Exploring CP12-binding proteins revealed aldolase as a new partner for the phosphoribulokinase/glyceraldehyde 3-phosphate dehydrogenase/CP12 complex. Purification and kinetic characterization of this enzyme from *Chlamydomonas reinhardtii*. *FEBS J.* **275**, 1248–1259
20. Jaquinod, M., Villiers, F., Kieffer-Jaquinod, S., Hugouvieux, V., Bruley, C., Garin, J., and Bourguignon, J. (2007) A proteomics dissection of *Arabidopsis thaliana* vacuoles isolated from cell culture. *Mol. Cell. Proteomics* **6**, 394–412
21. Ferro, M., Brugière, S., Salvi, D., Seigneurin-Berny, D., Court, M., Moyet, L., Ramus, C., Miras, S., Mellal, M., Le Gall, S., Kieffer-Jaquinod, S., Bruley, C., Garin, J., Joyard, J., Masselon, C., and Rolland, N. (2010) AT_CHLORO, a comprehensive chloroplast proteome database with subplastidial localization and curated information on envelope proteins. *Mol. Cell. Proteomics* **9**, 1063–1084
22. Dupieris, V., Masselon, C., Court, M., Kieffer-Jaquinod, S., and Bruley, C. (2009) A toolbox for validation of mass spectrometry peptides identification and generation of database IRMa. *Bioinformatics* **25**, 1980–1981
23. Raunser, S., Magnani, R., Huang, Z., Houtz, R. L., Trievel, R. C., Penczek, P. A., and Walz, T. (2009) Rubisco in complex with Rubisco large subunit methyltransferase. *Proc. Natl. Acad. Sci. U.S.A.* **106**, 3160–3165
24. Peltier, J. B., Cai, Y., Sun, Q., Zabrouskov, V., Giacomelli, L., Rudella, A., Ytterberg, A. J., Rutschow, H., and van Wijk, K. J. (2006) The oligomeric stromal proteome of *Arabidopsis thaliana* chloroplasts. *Mol. Cell. Proteomics* **5**, 114–133
25. Zybaïlov, B., Rutschow, H., Friso, G., Rudella, A., Emanuelsson, O., Sun, Q., and van Wijk, K. J. (2008) Sorting signals, N-terminal modifications, and abundance of the chloroplast proteome. *PLoS One* **3**, e1994
26. Berthiaume, L., Loisel, T. P., and Sygusch, J. (1991) Carboxyl-terminal region modulates catalytic activity of recombinant maize aldolase. *J. Biol. Chem.* **266**, 17099–17105
27. Finkemeier, I., Laxa, M., Miguet, L., Howden, A. J., and Sweetlove, L. J. (2011) Proteins of diverse function and subcellular location are lysine acetylated in *Arabidopsis*. *Plant Physiol.* **155**, 1779–1790
28. Trievel, R. C., Flynn, E. M., Houtz, R. L., and Hurley, J. H. (2003) Mechanism of multiple lysine methylation by the SET domain enzyme Rubisco LSM1. *Nat. Struct. Biol.* **10**, 545–552
29. Blom, N., and Sygusch, J. (1997) Product binding and role of the C-terminal region in class I D-fructose 1,6-bisphosphate aldolase. *Nat. Struct. Biol.* **4**, 36–39
30. Haake, V., Zrenner, R., Sonnewald, U., and Stitt, M. (1998) A moderate decrease of plastid aldolase activity inhibits photosynthesis, alters the levels of sugars and starch, and inhibits growth of potato plants. *Plant J.* **14**, 147–157
31. Haake, V., Geiger, M., Walch-Liu, P., Engels, C., Zrenner, R., and Stitt, M. (1999) Changes in aldolase activity in wild-type potato plants are important for acclimation to growth irradiance and carbon dioxide concentration, because plastid aldolase exerts control over the ambient rate of photosynthesis across a range of growth conditions. *Plant J.* **17**, 479–489
32. Stitt, M., Lunn, J., and Usadel, B. (2010) *Arabidopsis* and primary photosynthetic metabolism, More than the icing on the cake. *Plant J.* **61**, 1067–1091
33. Uematsu, K., Suzuki, N., Iwamae, T., Inui, M., and Yukawa, H. (2012) Increased fructose 1,6-bisphosphate aldolase in plastids enhances growth and photosynthesis of tobacco plants. *J. Exp. Bot.*, in press
34. Graciet, E., Lebreton, S., and Gontero, B. (2004) Emergence of new regulatory mechanisms in the Benson-Calvin pathway via protein-protein interactions. A glyceraldehyde-3-phosphate dehydrogenase/CP12/phosphoribulokinase complex. *J. Exp. Bot.* **55**, 1245–1254
35. Baginsky, S., and Gruissem, W. (2009) The chloroplast kinase network. New insights from large scale phosphoproteome profiling. *Mol. Plant* **2**, 1141–1153
36. Raines, C. A. (2011) Increasing photosynthetic carbon assimilation in C3 plants to improve crop yield. Current and future strategies. *Plant Physiol.* **155**, 36–42

**Characterization of Chloroplastic Fructose 1,6-Bisphosphate Aldolases as
Lysine-methylated Proteins in Plants**

Morgane Mininno, Sabine Brugière, Virginie Pautre, Annabelle Gilgen, Sheng Ma,
Myriam Ferro, Marianne Tardif, Claude Alban and Stéphane Ravanel

J. Biol. Chem. 2012, 287:21034-21044.

doi: 10.1074/jbc.M112.359976 originally published online April 30, 2012

Access the most updated version of this article at doi: [10.1074/jbc.M112.359976](https://doi.org/10.1074/jbc.M112.359976)

Alerts:

- [When this article is cited](#)
- [When a correction for this article is posted](#)

[Click here](#) to choose from all of JBC's e-mail alerts

Supplemental material:

<http://www.jbc.org/content/suppl/2012/04/30/M112.359976.DC1>

This article cites 34 references, 12 of which can be accessed free at
<http://www.jbc.org/content/287/25/21034.full.html#ref-list-1>